AAPS PharmSciTech (2022) 23:137
https://doi.org/10.1208/s12249-022-02283-z

RESEARCH ARTICLE

Transformation of Ritonavir Nanocrystal Suspensions into a Redispersible Drug Product via Vacuum Drum Drying

Barbara V. Schönfeld[1,2] · Ulrich Westedt[2] · Benjamin-Luca Keller[2] · Karl G. Wagner[1]

Received: 14 February 2022 / Accepted: 18 April 2022

Abstract
The present study explored vacuum drum drying (VDD) as potential drying technique for the solidification of crystalline ritonavir nanosuspensions prepared by wet-ball milling. In detail, the impact of drying protectants (mannitol, lactose, trehalose) added to the ritonavir nanosuspension was assessed in dependence of the drum temperature with respect to processibility via VDD, resulting intermediate powder properties, remaining nanoparticulate redispersibility and crystallinity. A clear impact of the glass transition temperature (T_g) of the drying protectant on the redispersibility/crystallinity of the VDD intermediate was observed. Increased T_g of the drying protectant was associated with improved redispersibility/crystallinity at a defined drum temperature. Consequently, the high T_g-substance trehalose and lactose showed a better performance than mannitol at higher drum temperatures. However, the processability and related powder properties were not in accordance with this observation. Mannitol containing formulations showed superior processibility to those containing trehalose/lactose. Moreover, the impact of the tableting and encapsulation process on the redispersibility of the VDD intermediate was studied for a selected formulation. Neither process demonstrated a negative impact on redispersibility. In conclusion, vacuum drum drying is a promising drying technique for the solidification of nanosuspensions to result in dried powder still containing ritonavir nanoparticles while demonstrating acceptable to good downstream processibility to tablets/capsules.

KEY WORDS ritonavir · vacuum drum drying · solidification · nanocrystals · drying protectants

INTRODUCTION

The importance of addressing the poor water-solubility of drug candidates in pharmaceutical development has become more pronounced in the last years, since nearly 90% of the drug candidates are poorly soluble, resulting in limited bioavailability (1–3). One strategy to tackle the solubility issue is the nanocrystal approach, whereby the crystalline drug substance is nanosized to improve dissolution behavior and saturation solubility according to the Noyes-Whitney and Ostwald-Freundlich principles (4–6). The nanocrystal formulations are generally based on a liquid, aqueous nanocrystal suspension (nanosuspension) in the nanometer size range (100–1000 nm). However, nanoparticles in aqueous media require stabilization since nanoparticles are much less stable than microparticles due to the Gibbs free energy contribution. Two types of stabilizers with different functional principles are described in literature: ionic stabilizers via thermodynamic/electrostatic stabilization, and steric stabilizers via kinetic stabilization (7, 8). The combination of both is most commonly utilized, demonstrating the highest stabilization effectiveness due to a synergistic effect which is also referred to as electrosteric stabilization (9–11).

Nanosuspensions can be prepared by either top-down (e.g., wet ball milling) or bottom-up (e.g., precipitation) approaches (12, 13). However, in the pharmaceutical industry, top-down approaches are far more relevant due to their simplicity, reproducibility and scalability (9, 13). The most prominent methods are NanoCrystal®

✉ Karl G. Wagner
karl.wagner@uni-bonn.de

[1] Department of Pharmaceutical Technology, University of Bonn, Gerhard-Domagk-Straße 3, 53121 Bonn, Germany

[2] AbbVie Deutschland GmbH & Co. KG, Knollstraße 50, 67061 Ludwigshafen, Germany

(wet ball milling) and IDD-P™ (insoluble drug delivery microparticle technology, high pressure homogenisation) (13) which are used in the manufacture of drug products such as Invega® Sustenna™ (Paliperidone palmitate via NanoCrystal®, Janssen 2009) or Triglide® (Fenofibrate via IDD-P™, Sciele Pharma, Skye Pharma 2005) (9).

Nanocrystals in aqueous suspensions are still associated with a certain risk of instabilities, either physical (e.g., Ostwald ripening and agglomeration), chemical (e.g., hydrolysis), or a risk for microbial growth leading to limited product shelf life (14–16). Another disadvantage of the administration of nanosuspensions as a liquid dosage form is the error-prone dosing step for patients, which may affect patient compliance and trigger the need for dosing devices. These disadvantages can be overcome by transforming the liquid nanocrystal suspension into a solid dosage form such as tablets or powder filled capsules. State-of-the-art solidification (drying) techniques include spray-drying, spray-coating (also termed spray granulation), and freeze drying (11–13).

In general, drying is a critical and essentially destabilizing procedure for the nanocrystal system which may lead to particle agglomeration and/or aggregation as well as crystal growth followed by sedimentation or flocculation. Consequently, redispersibility of nanoparticles upon reconstitution of the dried powder could be affected, which in turn reduces the beneficial effect of nanosizing on dissolution. For this reason, drying protectants are usually added to the final nanosuspension prior to the drying process to avoid particle growth. Common drying protectants include soluble sugars, such as lactose, sucrose or trehalose, or sugar alcohols like mannitol (14, 17). However, no nanocrystal-based drug product was approved by the FDA from 2009 to 2018 although drying protectants enable processability (9). This demonstrates how challenging and less economically efficient the common drying processes for solidification of nanocrystal suspensions are compared to other enabling technologies such as solid dispersion technology for solubility enhancement. This is particularly relevant in light of the observation that nanosizing technology is frequently used for early toxicology studies supply, which would be a straightforward approach for FIH development. Recently, vacuum drum drying (VDD) has been introduced as alternative approach to manufacture amorphous solid dispersions showing benefits especially compared to spray drying (18, 19). This technology is well-established in the food industry, but rarely known in the development of pharmaceuticals (20). The manufacture of ASDs as one enabling formulation principle consists of the embedment of the drug substance molecularly dispersed (i.e., amorphous) in a matrix polymer. Using vacuum drum drying as technology requires the dissolution of the drug substance and respective excipients in a common organic solvent.

In contrast, the nanocrystal approach essentially bases on the size reduction of a crystalline drug substance into nanosized particles (nanocrystals) in aqueous media followed by a solidification (drying) step. Consequently, the focus of the present case study was to investigate the suitability of vacuum drum drying as solidification (drying) technique for nanosuspensions with the potential to overcome obstacles and disadvantages of currently available drying technologies by, e.g., not needing a secondary drying step and by showing no viscosity related limitations for the solution to be dried and potentially higher yields. Thus, the suitability of vacuum drum drying for another enabling formulation principle, entirely different to the ASD approach, was examined to broaden the applicability in the pharmaceutical development.

The nanosuspension analyzed in this study consisted of ritonavir as model drug substance, sodium dodecyl sulfate as ionic stabilizer, and copovidone as steric stabilizer. More detailed, the impact of the drying protectant (mannitol, lactose, trehalose) on the processibility via VDD, on the dried powder properties, the remaining nanoparticulate redispersibility and crystallinity was assessed in dependence of the drum temperature. Subsequently, the most promising formulation was selected for further downstream processibility evaluation, with a particular focus on redispersibility. Therefore, the impact of compaction pressures during tableting was investigated as well as the impact of the encapsulation process on a pilot scale machine.

MATERIAL AND METHODS

Materials

Ritonavir (RTV, purity > 99.8%) was obtained from AbbVie Inc. (North Chicago, USA). Copovidone (polyvinylpyrrolidone–vinyl acetate copolymer, Kollidon® VA 64, COP) was purchased from BASF SE (Ludwigshafen, Germany), sodium dodecyl sulfate (SDS), mannitol (Parteck M 200 Emprove® Essential) and trehalose dihydrate (Emprove® Expert) from Merck KGaA (Darmstadt, Germany), and lactose (InhaLac®140) from MEGGLE Pharma (Wasserburg am Inn, Germany). Zirconium oxide beads were obtained from NETZSCH (Selb, Germany). Capsules (Quali-V HPMC capsules, size 0, color opaque grey) were purchased from Qualicaps (Madrid, Spain).

Methods

Preparation of Ritonavir Nanosuspensions by Wet Ball Milling

The ritonavir nanosuspension was prepared by wet ball milling (top-down approach, batch sizes 1.50–1.85 kg). Ritonavir (15% w/w) and 0.5 mm zirconium oxide beads as grinding

media (bead to ritonavir ratio: 1:18) were added to a stabilizer-containing solution (SDS (1% w/w) and copovidone (3% w/w)) into a 5-L HDPE (high-density polyethylene) bottle. The nanosizing was performed using a tumble blender (Turbula blender T10B, Willy A. Bachofen AG Maschienenfabrik, Muttenz, Switzerland) at 45 rpm for 69 h. Then, the zirconium beads were separated via filtration using a sieve with 200 µm mesh size. Prior to vacuum drum drying, drying protectants (mannitol, lactose, or trehalose; amount: 7.5%, 10%, 15%, or 25% w/w (see Table I)) as well as copovidone (7% w/w) were added to the ritonavir nanosuspension while stirring on a magnetic stirrer (IKA GmbH & Co KG, Staufen, Germany). Copovidone was added to increase the viscosity of the liquid formulation (drying dispersion) and thus, to increase the adhesion of the solution to the drums.

The nanosuspension formulation and the liquid formulations (drying dispersions) including drying protectant and copovidone were selected based on prior knowledge and formulation screening data (data not shown). The drying protectants investigated in the present study are commonly used excipients in the solidification of crystalline nanosuspensions (see "Introduction").

Characterization of Nanosuspensions

Particle Size Analysis by Dynamic Light Scattering Dynamic light scattering (DLS) method was applied using a Zetasizer Ultra (Malvern Instruments GmbH, Herrenberg, Germany) to determine the *z*-average and the polydispersity index (PDI) of the nanosuspensions after wet-ball milling. *z*-average represents the hydrodynamic diameter, and PDI expresses the width of the particle size distribution. The samples were diluted in water (1:20), and polystyrene single-use cuvettes (DTS0012) were used. The measurements were performed in back scatter mode (173°) as triplicates at 25°C prior to an equilibration time of 120 s. The results were analyzed using ZS Xplorer software (version 1.3.2.27).

Particle Size Analysis by Laser Diffraction Laser diffraction particle size analyzer (Mastersizer 3000, Malvern Instruments GmbH, Herrenberg, Germany) equipped with the automated dispersion unit "HydroMV" module was used to determine the particle size distribution of the nanosuspensions. For the measurements, nanosuspension was added to water until a laser obscuration of approximately 2–2.5% was reached. Data were analyzed according to the MIE theory using the Mastersizer 3000 Software (version 3.71). Measurements were performed as triplicates and averaged.

Solidification via Vacuum Drum Drying

The liquid formulations (drying dispersion: ritonavir nanosuspension + drying protectant + copovidone) were dosed into the gap of the two drums of the vacuum double drum dryer (Buflovak, New York, USA) for solidification. A thin film spread out evenly on the heated, counter-rotating drums covering full drum width. The water fraction of the liquid formulation (drying dispersion) evaporated during contact with the heated drums under vacuum conditions. The dried product was scraped off the drums by knifes showing

Table I Overview of Formulations Processed via VDD Incl. Drum Temperatures and Associated Short Names

Formulation composition of drying dispersion (liquid formulation)	Drum temperature (°C)	Ritonavir content in dried product (w/w%)	Short name
83% (w/w) RTV NS +10% (w/w) Man +7% (w/w) COP	75	38	Man10_75
78% (w/w) RTV NS +15% (w/w) Man +7% (w/w) COP	55	32	Man15_55*
78% (w/w) RTV NS +15% (w/w) Man +7% (w/w) COP	65	32	Man15_65
78% (w/w) RTV NS +15% (w/w) Man +7% (w/w) COP	75	32	Man15_75
68% (w/w) RTV NS +25% (w/w) Man +7% (w/w) COP	75	23	Man25_75
78% (w/w) RTV NS +15% (w/w) Lac +7% (w/w) COP	75	32	Lac15_75*
78% (w/w) RTV NS +15% (w/w) Lac +7% (w/w) COP	85	32	Lac15_85
78% (w/w) RTV NS +15% (w/w) Lac +7% (w/w) COP	95	32	Lac15_95
78% (w/w) RTV NS +15% (w/w) Tre +7% (w/w) COP	75	32	Tre15_75*
78% (w/w) RTV NS +15% (w/w) Tre +7% (w/w) COP	90	32	Tre15_90
78% (w/w) RTV NS +15% (w/w) Tre +7% (w/w) COP	105	32	Tre15_105
78% (w/w) RTV NS +7.5% (w/w) Man +7.5% (w/w) Lac +7% (w/w) COP	75	32	Man7.5/Lac7.5_75*
73% (w/w) RTV NS +10% (w/w) Man +10% (w/w) Lac +7% (w/w) COP	75	21	Man10/Lac10_75
78% (w/w) RTV NS +7.5% (w/w) Man +7.5% (w/w) Tre +7% (w/w) COP	75	32	Man7.5/Tre7.5_75*
73% (w/w) RTV NS +10% (w/w) Man +10% (w/w) Tre +7% (w/w) COP	75	21	Man10/Tre10_75

RTV NS ritonavir nanosuspension, *Man* mannitol, *Lac* lactose, *Tre* trehalose, *COP* copovidone, *VDD* vacuum drum drying

*Used for compression analysis

flake-like to powder-like appearance. The following process parameters were kept constant during drying for all formulations tested: casing temperature 80°C, pressure of 100 mbar, drum rotation speed 0.3 rpm, and drum gap 0.2 mm. The listed parameters were selected based on prior knowledge in the field of vacuum drum drying to result most likely in a dried product with reasonable quality properties. Since the solution to be dried was aqueous, the pressure was selected as low as applicable to ensure proper drying. The drum speed was set to a low value to increase the retention time of the product on the drums. In addition, a small drum gap was chosen, which effected the product thickness and thus, indirectly the required drying time. Just the drum temperature was varied in the range of 55 to 105°C for the formulations depending on the drying protectant used. The formulation-based adaption of the drum temperature ranges studied was chosen to consider the known differences in glass transition temperatures of the respective pure drying protectants (approximately 87–115°C) properly. The batch sizes were 350–500 g liquid formulation (drying dispersion) for small-scale runs and 1900 g for the large-scale run. Table I summarizes the formulations tested and the corresponding drum temperature during solidification.

The VDD intermediates of the small-scale runs were further processed into powder via manual sieving (mesh size 0.8 mm). For the large-scale evaluation, the VDD intermediate was milled at 2000 rpm using a screening mill (Comil U5, Quadro Engineering, Waterloo, Canada) equipped with an 813-µm round-hole sieve. The resulting powders of the small-scale runs were used for powder characterization and tableting, whereas the large-scale run was used for the encapsulation process.

Redispersibility of VDD Intermediates/Tablets/Capsules

For redispersibility evaluation, the VDD intermediates, tablets, or capsule-fillings were dispersed in an appropriate amount of water targeting the ritonavir concentration of the original nanosuspension (ritonavir: 15% w/w). The resulting suspension was mixed using a vortexer (IKA Vortexer VG3, Staufen, Germany) and subsequently characterized by laser diffraction and/or dynamic light scattering (see "Characterization of Nanosuspensions").

Redispersibility by Particle Fractions in Submicron Range The redispersibility was evaluated by means of laser diffraction to increase the understanding of the agglomeration state of the ritonavir particles, since larger particles could sediment during DLS analysis not being detected then. The percentage of particles below 1 µm in a cumulative volume-based particle size distribution was selected as criterion to determine the redispersibility.

Redispersibility Index For better comparability of the redispersed suspension with the initial nanosuspension, the redispersibility index (RDI) was calculated by normalizing the particle size describing variable (z-average or d_{50}) to the respective variable of the initial nanosuspension.

$$\mathrm{RDI} = \frac{\mathrm{d_{50}\ (or\ z-average)_{redispersed}}}{\mathrm{d_{50}(or\ z-average)_{initial}}} \quad (1)$$

Consequently, an RDI value close to 1 indicates a sufficient preservation of the nanoparticulate drug substance particles after solidification. For processability evaluation, the particle size describing variable of the tablets/capsule powder fill was compared with the respective one of the VDD intermediate (powder).

Characterization of VDD Intermediates

Bulk/Tapped Density Determination of bulk and tapped density was performed using tapped density tester (Pharmatest Apparatebau AG, Hamburg, Germany) according to Ph. Eur. 2.9.34 (method 1). VDD intermediate was filled into a 250-ml graduated cylinder and the mass and bulk/tapped volume occupied by the material was determined. All measurements were conducted as triplicates.

Flowability Determination of flow properties was performed using ring shear tester (RST-XS, Dietmar Schulze, Schüttgutmesstechnik, Wolfenbüttel, Germany) equipped with a 31.37-ml cell. VDD intermediates were measured as triplicates at following conditions: pre-shear normal stresses of 0.250, 0.525, 0.800, and 1 kPa, and ambient temperature (approximately 20–22°C). Data were evaluated using regression analysis.

Particle Size Distribution Determination of particle size distribution of VDD intermediates (powder) was performed using a laser diffraction particle size analyzer (Mastersizer 3000, Malvern Instruments GmbH, Herrenberg, Germany) equipped with a dry powder disperser module Aero S. The samples (approximately 2–5°g) were dispersed with 0 bar pressure and measured as triplicates. Data were analyzed using the Mastersizer 3000 Software (version 3.71) according to the Fraunhofer approximation.

Loss on Drying Determination of moisture content via loss on drying (LOD) method was performed using a halogen moisture analyzer (HB43-SSD, Mettler-Toledo GmbH, Giessen, Germany). The samples (approximately 5.5–6.1 g) were heated to 105°C and held until mass was constant within ± 1 mg for 100 s. The VDD intermediates were measured as triplicates.

Crystallinity and Glass Transition Temperature by Differential Scanning Calorimetry Quantification of ritonavir-related crystallinity as well as determination of the glass transition temperature ($T_{g,wet}$) was performed via differential scanning calorimetry (DSC) using a Mettler-Toledo DSC 3+ (Mettler Toledo, Gießen, Germany) equipped with an auto-sampler. All DSC samples (VDD intermediates) were scanned at 1.5 K/min from 25 to 140°C under nitrogen (gas flow 50 ml/min) as open pan method (crystallinity) and at 10 K/min from 25 to 150°C as closed pan method ($T_{g,wet}$). Pure crystalline ritonavir was measured (open pan method) to determine the melting enthalpy ($n = 2$, mean: 80.24 J/g) for quantification purposes of the VDD intermediates. The results were analyzed with STARe SW (version 16.1) (Mettler Toledo, Gießen, Germany). All VDD intermediate samples were measured as triplicates. The DSC thermograms are not shown in the present study except for Man7.5/Tre7.5_75_large representatively for all formulations in Figure OR1.

To verify the DSC results on quantification of the crystalline ritonavir content, powder X-ray diffraction (PXRD) was performed for one selected VDD intermediate (Man7.5/Tre7.5_75, see supplemental data).

Short-Term Stability Focusing on Redispersibility The physical stability of the selected VDD intermediate for downstream evaluation was determined by DLS and LD after storage for 2 and 6 months at uncontrolled conditions at room temperature and relative humidity (approximately 45–50%) and compared with initial nanosuspension data and initial powder characterization after solidification (drying).

Downstream Processability

Tabletability and Tableting For tabletability evaluation, round, biplane tablets (10 mm, mass: 200 mg, $n = 6$) of selected formulations (small-scale runs; see Table I) were manufactured using a single punch compression simulator (HB-50, Huxley Bertram Engineering Limited, Cambridge, UK) simulating a KorschXL100 (turret speed: 20 rpm, linear speed: 124 mm/s, dwell time: 78 ms). Different compaction pressures were applied targeting defined tensile strengths (0.4, 0.8, 1.2, 1.6, 2.0 MPa). The tensile strength range was selected around the commonly targeted tensile strength of 1.2 MPa for tablets (21). Tablets were subsequently analyzed regarding tablet weight (analytical balance, Sartorius BP 61 S-0CE, Sartorius AG, Goettingen, Germany), thickness and diameter (caliper, Hommel Hercules Werkzeughandel GmbH & Co. KG, Viernheim, Germany), and breaking force (ErwekaTBH 125, Erweka GmbH, Heusenstamm, Germany).

Encapsulation The selected VDD intermediate (Man7.5/Tre7.5_75; large-scale run) was encapsulated into size 0 Quali-V capsules in opaque grey targeting a fill weight of 157.2 mg (corresponding to 50 mg ritonavir). Encapsulation process was performed using an automated capsule filling machine (Modu-C LS, Harro Höfliger, Allmersbach im Tal, Germany) equipped with an inline in-process (weight) control unit. Process parameters were set as follows: 20 cycles/min, 100% check weighing (net weight). In-process control samples were taken at start, middle, and end of the encapsulation process and evaluated according to Ph. Eur. 2.9.5 (uniformity of mass of single-dose preparation). In addition, a process sample ($n = 100$) was taken and analyzed (gross weight). The machine protocol was used for process assessment (net weight).

Disintegration Disintegration test was performed according to Ph. Eur. 2.9.1 (test setup A) using a disintegration tester (ZT 722, Erweka GmbH, Heusenstamm, Germany).

RESULTS

Characterization of Ritonavir Nanosuspensions

Wet ball milling of ritonavir was successfully conducted in 5 sub-batches (runs) at different batch sizes (1.5–2.0 kg). The particle size analysis results are shown in Figure 1. The *z*-average values determined via dynamic light scattering (DLS) were below 400 nm (in a range of 300–370 nm), and the PDIs were below 0.15 indicating monodispersed ritonavir nanosuspensions (see Figure 1a). Laser diffraction (LD) analysis confirmed the DLS results showing the absence of large particles (e.g., agglomerates), which could be potentially missed via DLS due to sedimentation. The d_{50} values obtained by LD were in a range between 113 and 315 nm and more than 98.5% of the particles were in the submicron range (<1 µm) (see Figure 1b).

Solidification via VDD and Characterization of Resulting Intermediates

Impact of Drying Protectant and Drum Temperature on Processability

A clear dependency of the drying protectant used on processability could be observed as shown in Table II. Yield values were consistently low for lactose-containing formulations ranging from 53 to 62%. Mannitol-containing formulations showed yield values of 65–86% indicating a better process performance compared to lactose-containing formulations, whereas trehalose-containing formulations showed a pronounced drum temperature dependence: the higher the drum temperature, the better the yield (75°C: 63.3%, 105°C: 92.8%). Combining mannitol with either lactose or trehalose

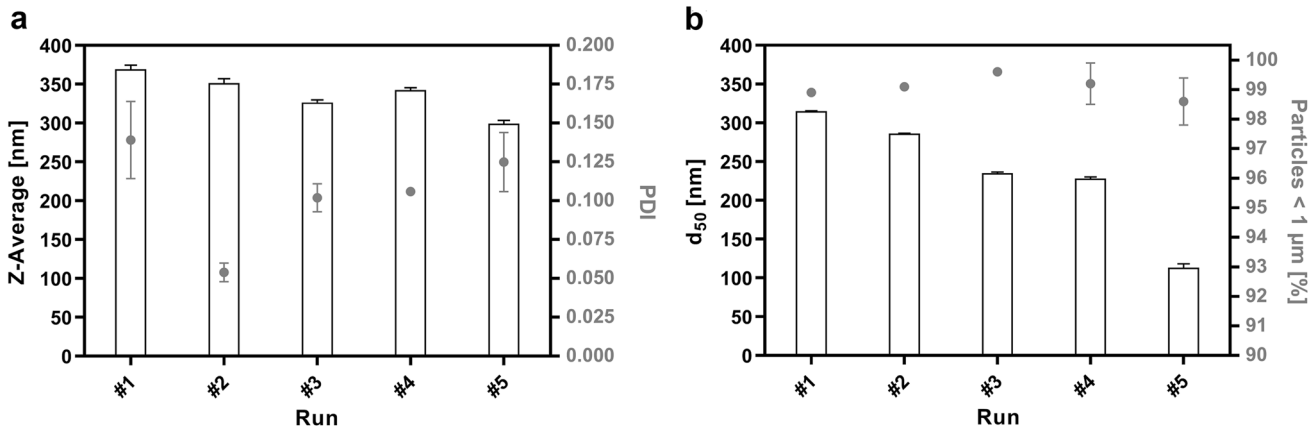

Fig. 1 Mean particle size results of ritonavir nanosuspensions (wet-ball milling runs 1–5); **a** dynamic light scattering–*z*-average and polydispersity index (PDI); **b** laser diffraction–d_{50} and number of particles below 1 µm in %

as drying protectants resulted in formulations with acceptable yield values of 65–87% for small-scale runs on a pilot scale VDD. The LOD values were between 1 and 3% for all other formulations except for the trehalose formulation (processed at 75°C with LOD of 4.90%) and the mannitol formulation (processed at 55°C with LOD of 4.87%).

Impact of Drying Protectant and Drum Temperature on Powder Properties of Dried Intermediates

Dried VDD intermediates have been characterized with respect to flowability (ring shear analysis), powder density (bulk/tapped), and solid particle size distribution (PSD). The results are summarized in Table II. The results indicated an impact of drying protectant type on flowability. All mannitol containing formulations exhibited easy flowing properties, whereas the lactose or trehalose containing powders showed cohesive flow independent of the drum temperature. Flow function coefficient values (FFC) for trehalose containing formulations indicated cohesive flow at lower temperatures and borderline easy flow at the highest drum temperature.

The bulk density values (Table II) were most favorable for further downstream processing for mannitol containing formulations with values at around 0.30–0.46 g/cm^3. The lactose and trehalose containing formulations showed lower bulk density ranging from 0.11 to 0.17 g/cm^3 indicating a fluffy powder. The formulations with two drying protectants, either mannitol/lactose (Man7.5/Lac7.5_75: 0.35 g/cm^3) or mannitol/trehalose (Man7.5/Tre7.5_75: 0.35 g/cm^3), resulted in powders with bulk density values in the same ranges of the pure mannitol containing formulation (Man15_75: 0.34 g/cm^3). Consequently, mannitol might be the dominant component within the formulation with respect to bulk density. This could be confirmed by the results of mannitol containing formulations at different mannitol levels: the higher the mannitol content within the dried product, the higher the bulk density: The bulk density for Man10_75 was 0.30 g/cm^3, that for Man15_75 was 0.34 g/cm^3, and the one for Man25_75 was 0.46 g/cm^3. For mannitol and lactose containing formulations, a minor dependence between drum temperature and bulk density values could be observed: the lower the drum temperature, the higher the bulk density. For trehalose, no trend could be observed.

The particle size distribution of the intermediates indicated relatively large particles of d_{90} values even above 1000 µm due to the selected sieve. However, trehalose and lactose containing intermediates tended to lower d_{90} values at around 600–650 µm for trehalose and 535–844 µm for lactose compared to mannitol (981–1120 µm). In addition, the mannitol level within the formulation impacted the d_{90} value: the higher the mannitol content, the higher the d_{90} value (Man10_75: 796 µm; Man15_75: 981 µm, Man25_75: 1330 µm). Furthermore, mannitol seemed to substantially impact the particle size distribution when combined with other drying protectants. The d_{50} and d_{90} values for Man7.5/Lac7.5_75 (d_{50}: 425 µm, d_{90}: 1170 µm) and Man7.5/Tre7.5_75 (d_{50}: 371 µm, d_{90}: 1030 µm) were widely comparable to those of Man15_75 (d_{50}: 388 µm, d_{90}: 981 µm).

Impact of Drying Protectant and Drum Temperature on Redispersibility

The impact of the drying protectant (mannitol, lactose, trehalose) at a defined amount (15% w/w within the liquid formulation (drying dispersion)) was assessed with respect to particle size and PDI after redispersing the VDD intermediate (redispersibility) dried at various drum temperatures via LD. Process conditions and the results are summarized in Table II. A clear trend could be observed for all three drying protectants investigated: with increasing drum temperature, the number of particles in the submicron range decreased, and the RDI increased indicating particle agglomeration/

Table II Results of Drying of Ritonavir Nanosuspension Formulations and Respective Vacuum Drum Dried Intermediates *(Man = Mannitol, Lac = Lactose, Tre = Trehalose, DL = Drug Load, FFC = Flow Function Coefficient, RDI = Redispersibility Index, T_g = Glass Transition Temperature)*

Formulation code	Yield (%)	Loss on drying (%)	Crystallinity in comp. to DL (%)	$T_{g,wet}$ (°C)	FFC	Bulk density (g/cm^3)	Tapped density (g/cm^3)	Particle size distribution (dried powder)			Particles < 1 µm (%) (liquid)	RDI (d_{50}, liquid)
								d_{10} [µm]	d_{50} [µm]	d_{90} [µm]		
Man10_75	67.1	1.38 ± 0.07	79.7 ± 1.5	n.d.	6.96 ± 0.68 (easy flow)	0.302 ± 0.001	0.413 ± 0.001	122.0 ± 13.1	357.0 ± 34.5	796.0 ± 62.5	29.06 ± 0.69	16.8
Man15_55	65.2	4.87 ± 0.04	85.4 ± 3.7	24.4 ± 0.4	4.97 ± 0.25 (easy flow)	0.435 ± 0.003	0.558 ± 0.005	242.0 ± 28.3	564.0 ±36.3	1120.0 ± 59.9	95.03 ± 0.02	1.1
Man15_65	83.5	2.95 ± 0.05	59.7 ± 0.5	n.d.	7.86 ± 4.86 (easy flow)	0.417 ± 0.004	0.535 ± 0.011	117.0 ± 8.2	442.0 ± 27.2	1120.0 ± 33.8	59.44 ± 4.40	2.0
Man15_75	78.8	1.45 ± 0.06	57.1 ± 8.6	n.d.	9.00 ± 3.72 (easy flow)	0.336 ± 0.011	0.458 ± 0.019	102.0 ± 2.0	388.0 ± 3.8	981.0 ± 24.0	20.55 ± 0.36	19.1
Man25_65	86.2	0.96 ± 0.09	74.0 ± 6.1	n.d.	4.09 ± 0.26 (easy flow)	0.348 ± 0.002	0.460 ± 0.003	122.0 ± 6.9	383.0 ± 27.6	850.0 ± 34.5	56.95 ± 0.73	2.2
Man25_75	78.7	1.47 ± 0.20	75.3 ± 4.1	n.d.	6.66 ± 2.45 (easy flow)	0.458 ± 0.012	0.571 ± 0.004	168.0 ± 30.5	621.0 ±35.4	1330.0 ± 35.0	40.86 ± 2.67	13.4
Lac15_75	62.4	1.48 ± 0.07	77.5 ± 5.0	n.d.	3.77 ± 0.19 (cohesive)	0.140 ± 0.001	0.212 ± 0.002	90.5 ± 2.1	261.0 ± 13.4	535.0 ± 53.2	93.84 ± 0.23	1.1
Lac15_85	59.1	2.29 ± 0.06	75.6 ± 0.1	49.3 ± 0.3	3.16 ± 0.12 (cohesive)	0.124 ± 0.001	0.183 ± 0.004	118.0 ± 3.5	362.0 ± 18.0	743.0 ± 26.9	92.59 ± 0.39	1.2
Lac15_95	53.9	1.42 ± 0.03	58.2 ± 1.1	n.d.	3.14 ± 0.19 (cohesive)	0.105 ± 0.003	0.159 ± 0.003	119.0 ± 2.7	374.0 ± 5.9	844.0 ± 4.5	23.85 ± 5.30	175.7
Tre15_75	63.3	4.90 ± 0.08	76.0 ± 5.6	n.d.	3.31 ± 0.32 (cohesive)	0.140 ± 0.003	0.211 ± 0.001	98.7 ± 1.8	301.0 ± 10.1	608.0 ± 38.7	94.47 ± 1.07	1.1
Tre15_90	68.7	1.06 ± 0.17	67.6 ± 3.2	55.7 ± 0.4	3.60 ± 0.03 (cohesive)	0.116 ± 0.001	0.175 ± 0.007	84.6 ± 3.3	296.0 ± 14.7	650.0 ± 21.7	97.02 ± 0.41	1.2
Tre15_105	92.8	1.30 ± 0.05	36.6 ± 1.3	n.d.	4.04 ± 0.36 (easy flow)	0.169 ± 0.002	0.258 ± 0.002	49.5 ± 1.8	230.0 ± 12.7	600.0 ± 76.2	10.26 ± 0.19	396.6
Man7.5/ Lac7.5_75	86.7	1.00 ± 0.04	69.2 ± 0.9	n.d.	2.75 ± 0.72 (cohesive)	0.352 ± 0.002	0.499 ± 0.002	87.1 ± 6.6	425.0 ± 37.0	1170 ± 79.4	99.78 ± 0.05	1.0
Man10/ Lac10_75	64.6	1.86 ± 0.10	86.0 ± 4.9	n.d.	2.32 ± 0.17 (cohesive)	0.393 ± 0.001	0.541 ± 0.003	139.0 ± 10.8	509.0 ± 39.3	1210 ± 48.7	93.92 ± 0.27	1.0
Man7.5/ Tre7.5_75_ small	84.8	1.02 ± 0.10	75.1 ± 3.0	n.d.	2.98 ± 0.30 (cohesive)	0.347 ± 0.009	0.474 ± 0.002	95.1 ± 7.7	371 ± 20.5	1030 ± 7.8	98.12 ± 0.15	1.0
Man7.5/ Tre7.5_75_ large	n.d.	0.89 ± 0.10	73.1 ± 0.8	n.d.	4.72 ± 0.82 (easy flow)	0.347 ± 0.004	0.483 ± 0.002	57.3 ± 2.3	193.0 ± 5.0	429.0 ± 5.6	99.81 ± 0.33	1.2
Man10/ Tre10_75	84.3	1.74 ± 0.04	90.1 ± 2.6	n.d.	2.73 ± 0.29 (cohesive)	0.333 ± 0.004	0.462 ± 0.001	121.0 ± 4.9	379.0 ± 4.7	864.0 ± 20.2	97.43 ± 0.17	1.1

n.d. not determined

crystal growth and thus, rated non-redispersible VDD intermediate. Consequently, a critical drum temperature (T_{crit}) could be identified at which the desired redispersibility of the dry VDD intermediate was still given (particles in submicron range >90% and RDI < 1.3). Figure 2 illustrates the T_{crit} and $T_{g,wet}$ for the respective formulations and the $T_{g,dry}$ of the pure drying protectants according to literature (12). A clear dependency between the $T_{g,dry}$ values of the respective drying protectants, the resulting formulation $T_{g,wet}$ values, and the T_{crit} values could be observed. Formulation Man15 with the lowest $T_{g,wet}$ showed the lowest T_{crit} (55°C) meaning that a redispersible intermediate is feasible at the lowest drum temperature tested. Consequently, applying drum temperatures above the T_{crit} during solidification would lead to a dried, less to non-redispersible product. In contrast, dried material with trehalose displayed the highest $T_{g,wet}$ value, and also the highest T_{crit} value with 90°C. However, the identified T_{crit} values were approximately 30–35°C above the wet $T_{g,wet}$ for all formulations.

Impact of Drying Protectant and Drum Temperature on Solid State of Ritonavir

Figure OR1 (Online Resource) displays the DSC thermograms of the pure microcrystalline ritonavir as reference for quantification of the remaining ritonavir-related crystallinity fraction ($n = 2$), and of the vacuum drum dried intermediate (Man7.5/Tre7.5_75_large) representative for all DSC measurements (data not shown). The crystalline fraction within the Man7.5/Tre7.5_75_large VDD intermediate was 23.2% corresponding to 73.0% remaining crystallinity. This is in accordance with the small-scale batch data (75.1%) of the same formulation. Additionally, an estimation of ritonavir-related crystallinity was determined via powder X-ray diffraction (PXRD) for the formulation Man7.5/Tre7.5_75_large. The remaining ritonavir-related crystallinity value was 89.93 % (see Figure OR2 (Online Resource)).

Figure 3 shows the impact of the drum temperature during vacuum drum drying on ritonavir-related crystallinity determined via DSC for formulations containing mannitol, lactose, or trehalose as drying protectant. Data indicate a dependency between drum temperature and ritonavir-related crystallinity: the higher the drum temperature for the respective formulation, the lower the crystalline ritonavir content within the VDD intermediate. A strong decrease in crystallinity could be observed for VDD intermediates processed at drum temperatures above T_{crit}. The crystallinity values at T_{crit} were in a range of 75–85%.

Short-Term Stability of Selected Formulation

The short-term stability study was carried out on the selected formulation Man7.5/Tre7.5_75 (see "Downstream Processability of Selected Formulation"). The VDD intermediate was analyzed after 2- and 6-month storage at uncontrolled conditions (room temperature; relative humidity of approximately 45–50%) using LD and/or DLS. Results were compared with VDD intermediate at study start (T0) and the corresponding nanosuspension. Results are given in Table III comprising the d_{50} values, the cumulative number of particles in the submicron range, and the z-average and PDI values. The d_{50} values ranged from 111 to 139 nm indicating no distinctive change over time regarding particle size. The number of particles in the submicron range were consistently above 97% and comparable to the corresponding nanosuspension with an initial value of 98.2%. However, z-average values indicated a slight shift to larger particles during storage: 299 nm (nanosuspension), 330 nm (after 2 months), and 353 nm

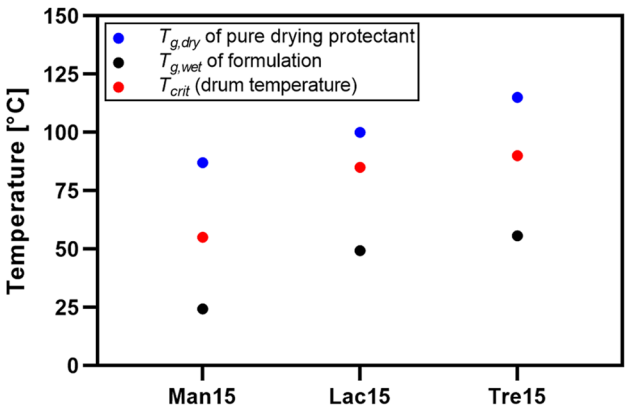

Fig. 2 Critical process (drum) temperature (T_{crit}) and glass transition temperature ($T_{g,wet}$) of formulations containing different drying protectants (mannitol, lactose, trehalose) and $T_{g,dry}$ of the pure drying protectants according to literature (12)

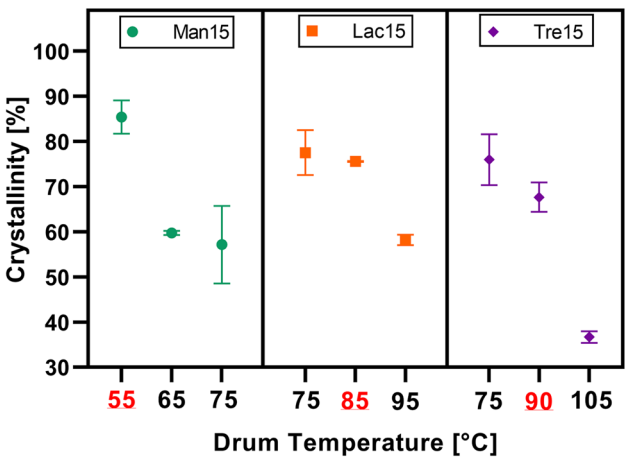

Fig. 3 Ritonavir-related crystallinity dependent on drum temperature of formulations containing mannitol (Man15), lactose (Lac15), and trehalose (Tre15) as drying protectant. Critical drying temperature (T_{crit}) for each formulation displayed in red

Table III Short-term stability results by laser diffraction and dynamic light scattering analysis at study start (T0), after 2 (T2) and 6 months (T6)

	Timepoint (months)			
	T0 (nanosuspension)	T0 (dried powder)	T2	T6
d_{50} (nm)	113.0 ± 5.2	130.0 ± 1.8	139.0 ± 0.8	111.0 ± 0.8
Particles <1 µm (%)	98.6 ± 0.8	98.4 ± 0.3	97.2 ± 0.0	98.4 ± 0.3
z-average (nm)	299.1 ± 4.30	Not determined	330.1 ± 6.98	352.5 ± 4.63
PDI[a]	0.125 ± 0.019	Not determined	0.119 ± 0.022	0.139 ± 0.003

[a]Polydispersibility index

(after 6 months). Consequently, it is recommended to store the dried product at lower temperatures and low humidity to avoid further particle agglomeration and/or crystal growth.

Downstream Processability of Selected Formulation

Formulation Man7.5/Tre7.5_75 was selected as prototype formulation to evaluate downstream processability comprising several benefits compared to other formulations tested. It showed good remaining nanoparticulate redispersibility, remaining crystallinity, and favorable powder properties such as bulk density (see Table II). The small-scale batch intermediate was used for tabletability evaluation to ensure proper comparability to the other formulations processed into powder intermediates using similar equipment (manually milled VDD intermediate). The large-scale batch intermediate was used for encapsulation experiments.

Tabletability and Disintegration of Selected Formulations

Figure 4a shows the tabletability plot (tensile strength *vs* compaction pressure) of selected formulations simulating the rotary press Korsch XL100 at 20 rpm turret speed (linear speed: 124 mm/s). All formulations were easily compressible leading to tablets with sufficient hardness even at low compaction pressures. Still, differences were observed depending on the drying protectant used in the formulation composition. Trehalose showed the best tabletability followed by lactose. Mannitol exhibited the least favored tabletability profile, but still showed sufficient tensile strength. Mannitol-containing formulations with lactose or trehalose in combination revealed comparable tabletability to the mannitol-only formulation. Consequently, mannitol affected tabletability most. Moreover, no tablet defects were observed for all formulations tested.

Figure 4b shows the impact of tensile strength on tablet disintegration for different formulations. All tablets showed fast disintegration time (< 12.5 min), which decreased with decreasing tensile strength.

Impact of Tableting Process on Redispersibility

Tablets of different formulations with a tensile strength of 1.2 MPa were investigated regarding redispersibility after tableting by laser diffraction. The results are summarized in Table IV. The d_{50} values of the redispersed tablets were similar to the initial VDD powder intermediates. RDI values of 1.0–1.1 indicated no substantial change in PSD of redispersed particles with a large number of particles (> 93%)

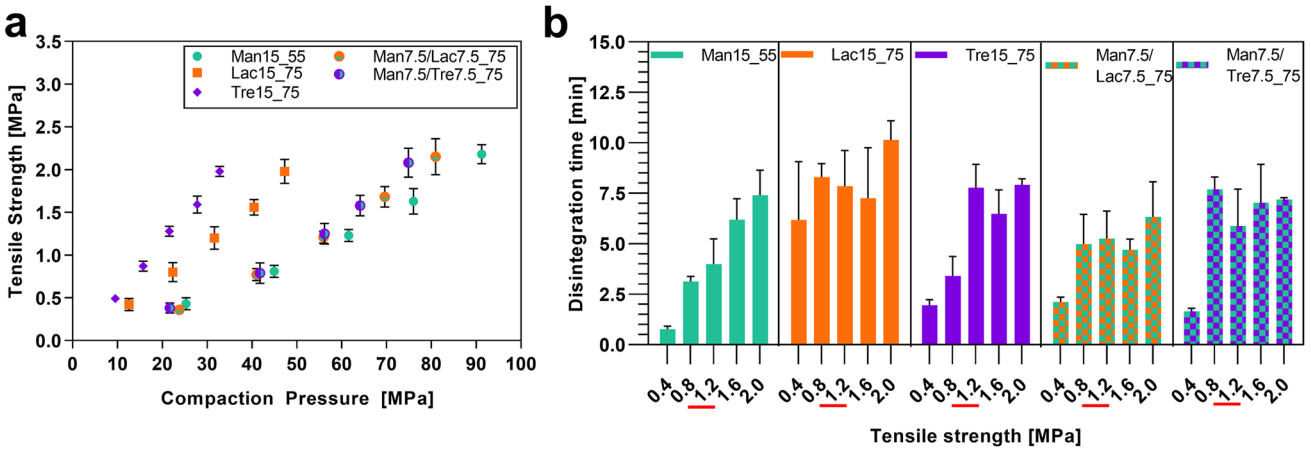

Fig. 4 **a** Tabletability plots of selected formulations simulating a Korsch XL100 at 20 rpm ($n = 6$); **b** Disintegration time of selected formulations compressed to tablets of defined tensile strengths ($n = 6$); Man = mannitol, Lac = lactose, Tre = trehalose

smaller than 1 µm. Consequently, no impact on tableting on redispersibility could be observed.

In addition, the impact of tableting on redispersibility was studied with tablets of different tensile strengths via DLS and LD for a selected formulation (Man7.5/Tre7.5_75). As shown in Figure 5, the *z*-average values by DLS were in a comparable range (342–367 nm) for all tensile strengths. Measured PDIs (0.100–0.175) indicated monodispersed nanosuspensions. RDI values of 1.0 to 1.1 demonstrated good redispersibility. LD results were in accordance with those from DLS measurements: the d_{50} values varied from 196 to 239 nm with 95.1–99.8% of the particles in the submicron range. The RDI values of LD measurement did not indicate any particle size change induced by the tableting process.

Impact of Encapsulation Process on Redispersibility

The selected VDD intermediate (Man7.5/Tre7.5_75) was successfully encapsulated into size 0 HPMC capsules targeting a fill weight of 157 mg (RTV dose of 50 mg). Approximately 1000 capsules were manufactured. The results of the analyzed in-process control and process samples combined with machine protocol data are summarized in Table OR2 (Online Resource) reflecting an acceptable encapsulation process.

Redispersibility of the capsule powder fill (powder) was assessed via DLS and LD for the in-process control samples (see Figure 6). The *z*-average values ranged from 320 to 333 nm and the PDI from 0.114 to 0.126 assuming monodispersed nanosuspensions. The RDI values were constantly at 1.0. The particle size analysis data via LD were in accordance with the DLS data: the d_{50} values were between 135 and 140 nm with 99% of the particles in the submicron range without variation with respect to processing time. And the RDI values were at 1.0 indicating no change in particle size compared to the VDD powder. Thus, the encapsulation process did not impact the remaining nanoparticulate redispersibility of the capsule powder fill.

Table IV Tablets (TS: 1.2 MPa) Redispersibility of Different Formulations by Laser Diffraction (*Man = Mannitol, Lac = Lactose, Tre = Trehalose, RDI = Redispersibility Index*)

Formulation	Particles < 1 µm (%)	RDI	Disintegration time (min)
Man15_55	92.67 ± 0.05	1.0	3.99 ± 1.25
Lac15_75	95.46 ± 0.23	1.0	7.86 ± 1.76
Tre15_75	93.26 ± 0.14	1.0	7.79 ± 1.14
Man7.5/Lac7.5_75	99.68 ± 0.72	1.0	5.25 ± 1.37
Man7.5/Tre7.5_75	96.47 ± 0.72	1.0	5.88 ± 1.83

DISCUSSION

Ritonavir nanocrystal suspensions could be successfully manufactured with good reproducibility via wet-ball milling using zirconium oxide beads using a classic tumble blender.

The data revealed that processibility of the tested nanocrystals containing liquid formulations (drying dispersions) during vacuum drum drying was impacted by the drying protectant. Mannitol was identified as best drying protectant for product solidification in terms of visual behavior on the drums, LOD, and yield. Similar observations were made by Chaubal, Popescu (12) comparing lactose, mannitol, sucrose, and dextrose containing spray dried powders of itraconazole nanosuspensions: mannitol was rated as most favorable carrier for spray drying of nanoparticles providing most desirable particle morphology, flowability, and LOD values.

The redispersibility was mostly affected by the interplay between drying protectant and drum temperature. An individual critical process temperature (T_{crit}) correlating with the

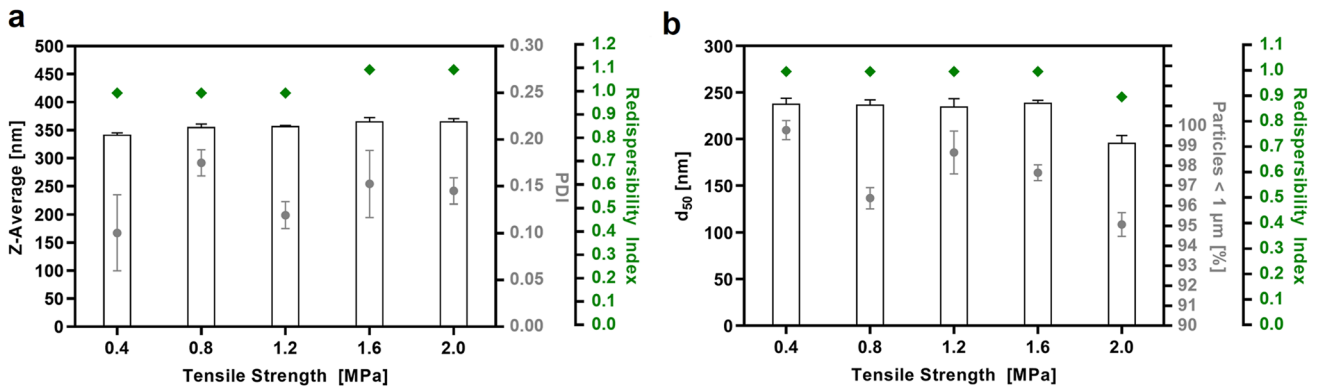

Fig. 5 Mean particle size results of tablets with different tensile strength values; **a** dynamic light scattering– *z*-average and polydispersity index (PDI); **b** laser diffraction– d_{50} and number of particles below 1 µm in %; RDI redispersibility index compared to powder

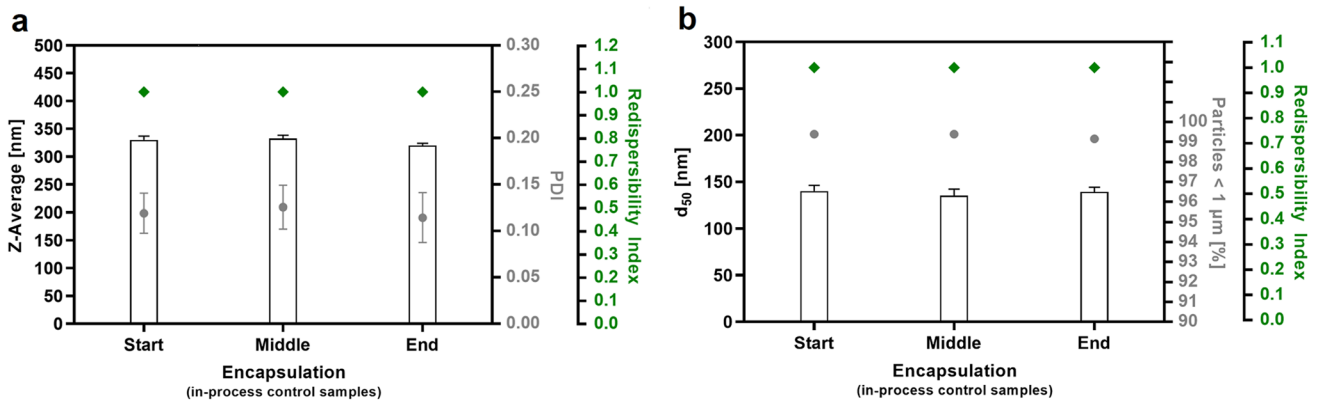

Fig. 6 Mean particle size results of in-process control samples of the encapsulation process; **a** dynamic light scattering– *z*-average and polydispersity index (PDI); **b** laser diffraction– d_{50} and number of particles below 1 µm in %; RDI redispersibility index compared to powder

$T_{g,wet}$ of the formulation could be identified for all formulations tested. Similar observations were recently published for the spray drying process by Czyz *et al.* (14). Researchers reported that the outlet temperature during spray drying seemed to be critical and correlated with the $T_{g,wet}$ of the formulation, which was shown to be drug load related. The temperature difference between $T_{g,wet}$ of the formulation and T_{crit} (outlet) was similar for all formulations tested (approximately 20–25°C). In the present study, the difference between $T_{g,wet}$ of the formulation and T_{crit} (drum) was 30–35°C and thus, approximately 10° higher compared to the spray drying data. This might be explained by the fact that the drum temperature did not reflect the product temperature, which is probably lower due to the cooling effect during water evaporation. In contrast, the outlet temperature during spray drying is much better linked to the real product temperature. Consequently, it can be assumed that a T_{crit} related to the $T_{g,wet}$ of the formulation might be process independent. An explanation for the temperature impact on redispersibility could be as follows: process temperatures above the $T_{g,wet}$ *o*f the material knowingly increase the fluidity of the material and potentially facilitate nanocrystals aggregation and growing. Interestingly, Malamatari *et al.* (22) identified the ratio of drying protectant to drug as another important formulation-related factor for redispersibility. The present study confirmed their findings, as the amount of submicron particles was increased at higher mannitol to ritonavir ratio (20% for Man15_75, 40% for Man25_75) at constant drum temperature. This stabilizing effect was likely caused by steric hindrance by the drying protectant. Zuo *et al.* explains this steric hindrance as follows: the presence of water-soluble additives such as Mannitol could form hydrophilic excipient bridges interconnecting the nanoparticles and thus, avoiding crystal-to-crystal contact and in the end crystal growth. The same stabilizing effect is seen in lyophilization processes where mannitol is used as so called lyo-protectant (23). Surprisingly, Man10_75 showed better redispersibility compared to Man15_75, despite containing a lower amount of drying protectant. In this case, the T_g impact would be more pronounced as stabilizing principle than the steric hindrance. Reducing the mannitol content resulted in a higher relative content of copovidone in the formulation, which has a higher $T_{g,dry}$ (101°C) compared to mannitol. Consequently, the $T_{g,wet}$ of the formulation might be higher and thus, leading to a higher stabilizing effect against temperature. In addition, copovidone acts as matrix polymer still providing sufficient stabilization. Hence, the stabilizing effect of drying protectants on the nanocrystals might be dominated by two principles: steric hindrance (acting as spacers by building excipient bridges) and T_g influence. However, other components of the formulation might influence the T_g significantly as well (e.g., drug substance, ionic or polymeric stabilizers or adhesion enhancers).

The remaining ritonavir-related crystallinity data determined via DSC showed a clear ritonavir melting peak visible in the thermograms of all analyzed samples. However, a temperature shift to a lower melting temperature was observed for the VDD intermediates containing ritonavir nanoparticles compared to the pure microcrystalline ritonavir measurements. Based on literature, melting point depression is expected with reduction of crystal particle size as described by the Gibbs-Thomson equation (24). In fact, this has been already reported for several nanosuspensions dried via spray drying in previously published studies (25, 26). Consequently, measuring the remaining crystallinity at nanometer size via DSC might potentially not reflect the true crystallinity. Few percent of crystallinity might get lost due to fast melting of nanocrystals at even lower temperatures which is also implied by the left skewed melting peak in the VDD intermediate thermograms. In fact, even PXRD data represent only an estimation, because a reference standard had to be used for quantification. Consequently, the true

crystallinity might be a bit higher compared to the estimated values by DSC in this study.

However, DSC data clearly indicated that a portion of the ritonavir was converted into a non-crystalline (most likely amorphous) form even at the lowest process (drum) temperatures. This observation was in accordance with the results of a recently published study, where a risperidone nanosuspension was processed by spray drying (27). Kayaert, Van den Mooter (28) stated that the cause of amorphization is most likely the interplay between drug and stabilizer during drying, rather than the nanosizing via wet-ball milling. Indeed, if the drug substance is soluble in the stabilizer, especially if the stabilizer is a polymer, it enhances the probability of an amorphous layer formed at the interface. In the present formulations, copovidone was used to increase the adhesion to the drums of the vacuum drum dryer, next to its function as polymeric stabilizer of the liquid nanosuspension. Consequently, the level of copovidone within the final dried intermediate was quite high (25% w/w) enabling the solubilization process of ritonavir. This solubilization was even more enhanced by the presence of nanocrystals instead of microcrystals. In addition, this study clearly showed a drum temperature dependency for the remaining crystallinity: the higher the drum temperature, the higher the amorph fraction. Interestingly, the critical drum temperature for remaining crystallinity corresponded with the T_{crit} value for redispersibility.

Since non-crystalline API, e.g., amorphous API, can recrystallize during storage (28), this partial change in solid state might have an impact on stability. Consequently, different solid states after manufacturing and after drying of the nanosuspension should be avoided to ensure stability as key design requirement. This might be even more critical for substances showing pronounced polymorphisms. Thus, future research should investigate the impact of non-crystalline API within a solidified nanocrystal drug product on storage stability.

The short-term stability evaluation of the present study indicated a slight increase in particle size determined via DLS (see Table III). However, an increase in particle size could not be detected via LD. Kumar *et al*. (29) found out that all indomethacin nano-formulations were stable after spray drying and during storage stability which contained small molecular weight sugars such as mannitol, lactose, and trehalose. However, the ratio between the drying protectant and API was much higher (1 to 5 w/w) compared to the formulation tested in this present study (1 to 1.3 w/w). A higher drying protectant to API ratio is known to be beneficial ensuring better steric stabilization, and thus, redispersibility as stated by Malamatari *et al*. (22). Yet, the API load would be significantly lower.

As mitigation concept for crystal growth/aggregation, stability, and amorphization, the T_g of the formulation should be determined prior to the drying step to choose the processing temperature, accordingly, meaning below the T_{crit} of the respective formulation. This applies presumably for both, spray drying and vacuum drum drying. However, the composition of the nanosuspension prior drying needs to be selected carefully considering the type of drying protectant, its T_g, and the ratio of drying protectant to API. Drying protectants with higher T_g might be preferred enabling lower drying protectant to API ratio, and thus, higher API loads of the final dosage form. Moreover, the solubility of the API within the polymeric stabilizer needs to be assessed to avoid unintended amorphization of the API.

The compression into tablets revealed a dependence on the drying protectant in the formulation. This might be related to the compression behavior of the neat drying protectant and the particle size and shape of the VDD intermediates. Nevertheless, all formulations showed acceptable tabletability, since resulting tablets exhibited sufficient tensile strength even at low compaction pressures.

Results from the redispersibility assessment indicated that tableting did not impact redispersibility for all formulations at a tensile strength of 1.2 MPa. This was surprising, since nanosized ritonavir particles were assumed to proximate to each other during the tableting process. But even at higher compaction pressures and higher tablet tensile strength respectively, only disintegration was affected, however, not redispersibility. Moreover, it could be demonstrated that encapsulation of VDD intermediate to capsules did not affect redispersibility of the final drug product.

To sum up, the drying process of a stabilized nanosuspension seems to be the most critical step during the manufacture of a nanocrystal drug product. The selection of the formulation components is important for several reasons. Selected excipients should enable the following:

- Stabilizing the liquid nanosuspension by preventing particle growth, agglomeration, and precipitation
- Enabling the spreading of the nanosuspension, and in turn ensure uniform drying on the heated drums
- Achieving acceptable flow and density of the dried and subsequently screened intermediate to ensure downstream processability for encapsulation or compression.

CONCLUSION

The present study demonstrated the feasibility of using vacuum drum drying (VDD) for the solidification of ritonavir nanosuspensions resulting in redispersible solids. VDD offers advantages for downstream processing. First, no second drying step is required. Second, the powder properties of the dried intermediate, such as particle size

distribution, can be adjusted during milling and by this, potentially optimized for subsequent encapsulation or compression into tablets, which was demonstrated for a selected model formulation.

Moreover, first insights were gathered on the interplay between formulation composition and VDD process conditions (drum temperature), on the resulting impact on powder redispersibility, and on the remaining ritonavir related crystallinity as follows:

- For all studied formulations redispersibility and DS-crystallinity substantially decreased exceeding a formulation specific drum temperature (T_{crit}).
- As T_{crit} is formulation dependent, it should be identified for each formulation as part of the process development.
- T_{crit} might be correlated with the glass transition temperature ($T_{g,wet}$) of the formulation, which is mostly dominated by the T_g of the pure drying protectant. However, this needs further mechanistic clarification.
- Particle growth during drying can be prevented by taking advantage of the principles of steric hindrance in combination with possibly high T_g of the formulation leading to less fluidity.
- As the stabilizers for the nanosuspension will affect the overall T_g, the type and amount should be carefully selected for formulation composition.

Supplementary Information The online version contains supplementary material available at https://doi.org/10.1208/s12249-022-02283-z.

Acknowledgements The authors kindly thank Stefan Weber (AbbVie Deutschland GmbH & Co. KG) for his support in powder X-ray diffraction and Harald Hach (AbbVie Deutschland GmbH & Co. KG) for his support during preparation of the formulations.

Author Contributions Barbara V. Schönfeld: conceptualization, methodology, investigation, visualization, writing — original draft. Benjamin-Luca Keller: conceptualization, methodology, writing — review and editing. Ulrich Westedt: conceptualization, methodology, project administration, supervision, writing — review and editing. Karl G. Wagner: conceptualization, methodology, supervision, writing — review and editing. The University of Bonn and AbbVie participated in study design, research, interpretation of data, writing, data collection, analysis, reviewing, and approving the publication.

Funding Open Access funding enabled and organized by Projekt DEAL. This work was funded by AbbVie Deutschland GmbH & Co. KG.

Declarations

Competing Interests Barbara V. Schönfeld, Benjamin-Luca Keller, and Ulrich Westedt are employees of AbbVie and may own AbbVie stock. Barbara V. Schönfeld is a PhD student, and Karl G. Wagner is a professor at the University of Bonn. They have no additional conflicts of interest to report.

References

1. Loftsson T, Brewster ME. Pharmaceutical applications of cyclodextrins: basic science and product development. J Pharm Pharmacol. 2010;62(11):1607–21. https://doi.org/10.1111/j.2042-7158.2010.01030.x.
2. Lipinski CA, Lombardo F, Dominy BW, Feeney PJ. Experimental and computational approaches to estimate solubility and permeability in drug discovery and development settings. Adv Drug Deliv Rev. 2001;46(1):3–26. https://doi.org/10.1016/S0169-409X(00)00129-0.
3. Khan KU, Minhas MU, Badshah SF, Suhail M, Ahmad A, Ijaz S. Overview of nanoparticulate strategies for solubility enhancement of poorly soluble drugs. Life Sci. 2022;291:120301. https://doi.org/10.1016/j.lfs.2022.120301.
4. Dolenc A, Kristl J, Baumgartner S, Planinšek O. Advantages of celecoxib nanosuspension formulation and transformation into tablets. Int J Pharm. 2009;376(1):204–12. https://doi.org/10.1016/j.ijpharm.2009.04.038.
5. Merisko-Liversidge E, Liversidge GG. Nanosizing for oral and parenteral drug delivery: a perspective on formulating poorly-water soluble compounds using wet media milling technology. Adv Drug Deliv Rev. 2011;63(6):427–40. https://doi.org/10.1016/j.addr.2010.12.007.
6. Müller RH, Peters K. Nanosuspensions for the formulation of poorly soluble drugs: I. Preparation by a size-reduction technique. Int J Pharm. 1998;160(2):229–37. https://doi.org/10.1016/S0378-5173(97)00311-6.
7. Liu P, Rong X, Laru J, van Veen B, Kiesvaara J, Hirvonen J, *et al*. Nanosuspensions of poorly soluble drugs: preparation and development by wet milling. Int J Pharm. 2011;411(1):215–22. https://doi.org/10.1016/j.ijpharm.2011.03.050.
8. Choi J-Y, Yoo JY, Kwak H-S, Uk Nam B, Lee J. Role of polymeric stabilizers for drug nanocrystal dispersions. Curr Appl Phys. 2005;5(5):472–4. https://doi.org/10.1016/j.cap.2005.01.012.
9. Jermain SV, Brough C, Williams RO. Amorphous solid dispersions and nanocrystal technologies for poorly water-soluble drug delivery — an update. Int J Pharm. 2018;535(1):379–92. https://doi.org/10.1016/j.ijpharm.2017.10.051.
10. Singhal M, Baumgartner A, Turunen E, van Veen B, Hirvonen J, Peltonen L. Nanosuspensions of a poorly soluble investigational molecule ODM-106: impact of milling bead diameter and stabilizer concentration. Int J Pharm. 2020;587:119636. https://doi.org/10.1016/j.ijpharm.2020.119636.
11. Lee J. Drug nano- and microparticles processed into solid dosage forms: physical properties. J Pharm Sci. 2003;92(10):2057–68. https://doi.org/10.1002/jps.10471.
12. Chaubal MV, Popescu C. Conversion of nanosuspensions into dry powders by spray drying: a case study. Pharm Res. 2008;25(10):2302–8. https://doi.org/10.1007/s11095-008-9625-0.

13. Möschwitzer JP. Drug nanocrystals in the commercial pharmaceutical development process. Int J Pharm. 2013;453(1):142–56. https://doi.org/10.1016/j.ijpharm.2012.09.034.
14. Czyz S, Wewers M, Finke JH, Kwade A, van Eerdenbrugh B, Juhnke M, *et al*. Spray drying of API nanosuspensions: importance of drying temperature, type and content of matrix former and particle size for successful formulation and process development. Eur J Pharm Biopharm. 2020;152:63–71. https://doi.org/10.1016/j.ejpb.2020.04.021.
15. Hou Y, Shao J, Fu Q, Li J, Sun J, He Z. Spray-dried nanocrystals for a highly hydrophobic drug: Increased drug loading, enhanced redispersity, and improved oral bioavailability. Int J Pharm. 2017;516(1):372–9. https://doi.org/10.1016/j.ijpharm.2016.11.043.
16. Van Eerdenbrugh B, Van den Mooter G, Augustijns P. Top-down production of drug nanocrystals: nanosuspension stabilization, miniaturization and transformation into solid products. Int J Pharm. 2008;364(1):64–75. https://doi.org/10.1016/j.ijpharm.2008.07.023.
17. Kesisoglou F, Panmai S, Wu Y. Nanosizing — oral formulation development and biopharmaceutical evaluation. Adv Drug Deliv Rev. 2007;59(7):631–44. https://doi.org/10.1016/j.addr.2007.05.003.
18. Schönfeld BV, Westedt U, Wagner KG. Vacuum drum drying — a novel solvent-evaporation based technology to manufacture amorphous solid dispersions in comparison to spray drying and hot melt extrusion. Int J Pharm. 2021;596:120233. https://doi.org/10.1016/j.ijpharm.2021.120233.
19. Schönfeld BV, Westedt U, Wagner KG. Compression of amorphous solid dispersions prepared by hot-melt extrusion, spray drying and vacuum drum drying. International Journal of Pharmaceutics: X 2021:100102. doi: https://doi.org/10.1016/j.ijpx.2021.100102.
20. Bhandari B, Bansal N, Zhang M, Schuck P. 4.1 Introduction. Handbook of food powders — processes and properties. Woodhead Publishing; 2013.
21. Vorländer K, Kampen I, Finke JH, Kwade A. Along the process chain to probiotic tablets: evaluation of mechanical impacts on microbial viability. Pharmaceutics. 2020;12(1):66. https://doi.org/10.3390/pharmaceutics12010066.
22. Malamatari M, Somavarapu S, Kachrimanis K, Buckton G, Taylor KMG. Preparation of respirable nanoparticle agglomerates of the low melting and ductile drug ibuprofen: impact of formulation parameters. Powder Technol. 2017;308:123–34. https://doi.org/10.1016/j.powtec.2016.12.007.
23. Wang W. Lyophilization and development of solid protein pharmaceuticals. Int J Pharm. 2000;203(1):1–60. https://doi.org/10.1016/S0378-5173(00)00423-3.
24. Jackson CL, McKenna GB. The melting behavior of organic materials confined in porous solids. J Chem Phys. 1990;93(12):9002–11. https://doi.org/10.1063/1.459240.
25. Medarević D, Djuriš J, Ibrić S, Mitrić M, Kachrimanis K. Optimization of formulation and process parameters for the production of carvedilol nanosuspension by wet media milling. Int J Pharm. 2018;540(1):150–61. https://doi.org/10.1016/j.ijpharm.2018.02.011.
26. Zhang X, Guan J, Ni R, Li LC, Mao S. Preparation and solidification of redispersible nanosuspensions. J Pharm Sci. 2014;103(7):2166–76. https://doi.org/10.1002/jps.24015.
27. Nair A, Khunt D, Misra M. Application of quality by design for optimization of spray drying process used in drying of Risperidone nanosuspension. Powder Technol. 2019;342:156–65. https://doi.org/10.1016/j.powtec.2018.09.096.
28. Kayaert P, Van den Mooter G. Is the amorphous fraction of a dried nanosuspension caused by milling or by drying? A case study with Naproxen and Cinnarizine. Eur J Pharm Biopharm. 2012;81(3):650–6. https://doi.org/10.1016/j.ejpb.2012.04.020.
29. Kumar S, Gokhale R, Burgess DJ. Sugars as bulking agents to prevent nano-crystal aggregation during spray or freeze-drying. Int J Pharm. 2014;471(1):303–11. https://doi.org/10.1016/j.ijpharm.2014.05.060.